J|A|C|S
ARTICLES
Published on Web 05/22/2002

The Reaction of Triplet Flavin with Indole. A Study of the Cascade of Reactive Intermediates Using Density Functional Theory and Time Resolved Infrared Spectroscopy

Christopher B. Martin, Meng-Lin Tsao, Christopher M. Hadad,* and Matthew S. Platz*

Contribution from the Department of Chemistry, The Ohio State University, 100 West 18th Avenue, Columbus, Ohio 43210

Received October 15, 2001. Revised Manuscript Received February 13, 2002

Abstract: As a model for riboflavin, lumiflavin was investigated using density functional theory methods (B3LYP/6-31G* and B3LYP/6-31+G**) with regard to the proposed cascade of intermediates formed after excitation to the triplet state, followed by electron-transfer, proton-transfer, and radical−radical coupling reactions. The excited triplet state of the flavin is predicted to be 42 kcal/mol higher in energy than the singlet ground state, and the π radical anion lies 45.1 kcal/mol lower in energy than the ground-state flavin and a free electron in the gas phase. The former value compares to a solution-phase triplet energy of 49.8 kcal/mol of riboflavin. For the radical anion, the thermodynamically favored position to accept a proton on the flavin ring system is at N_5. A natural population analysis also provided spin density information for the radicals and insight into the origin of the relative stabilities of the six different calculated hydroflavin radicals. The resulting 5H-LF• radical can then undergo radical−radical coupling reactions, with the most thermodynamically stable adduct being formed at $C_{4'}$. Vibrational spectra were also calculated for the transient species. Experimental time-resolved infrared spectroscopic data obtained using riboflavin tetraacetate are in excellent agreement with the calculated spectra for the triplet flavin, the radical anion, and the most stable hydroflavin radical.

I. Introduction

Riboflavin (vitamin B_2) is found in milk, beer, yeast, and leafy vegetables. It is an important part of a healthy diet.[1] Riboflavin (RB) is a yellow-orange compound which undergoes numerous reactions when exposed to solar radiation. In neutral aqueous solution, riboflavin forms lumichrome (LC) upon photolysis, and in alkaline solution, lumiflavin (LF) is produced.[2−4]

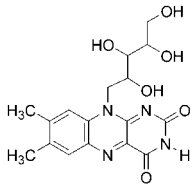

RB

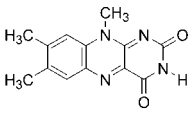

LF

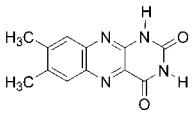

LC

Riboflavin is known to undergo photoreactions with nucleic acids[5−7] and to sensitize the killing of tumor cells[8] and intra- and extra-cellular HIV.[9]

Riboflavin undergoes complex photochemical reactions with proteins in vivo. Photolysis of RB in the lens of the eye leads to the formation of flavin-ocular protein adducts.[10,11] Photolysis of RB in plasma (which transpires when jaundiced newborns are treated for hyperbilirubinemia) produces a flavin-albumin adduct.[12−17] The structures of these adducts are not known, but it has been determined that tryptophan residues are involved in this linkage.[18] It seems likely that adduct formation involves the triplet state of the flavin because adduct formation is quenched by 10 mM ascorbate ion.[19]

* To whom correspondence should be addressed. E-mail (M.S.P.): platz.1@osu.edu. Fax: 614-292-1685. E-mail (C.M.H.): hadad.1@osu.edu. Fax: 614-292-1685.

(1) *The Merck Index*, 12th ed.; Budavari, S., Ed.; Merck Research Laboratories, Rahway, NJ, 1996; pp 956, 957, and 1410 and references therein.
(2) Heelis, P. F. *Chem. Soc. Rev.* **1982**, *11*, 15−39.
(3) Heelis, P. F. *Chem. Biochem. Flavoenzymes* **1991**, *1*, 171−193.
(4) Song, P.-S.; Metzler, D. E. *Photochem. Photobiol.* **1967**, *6*, 691−709.
(5) Ennever, J. F.; Carr, H. S.; Speck, W. T. *Pediatr. Res.* **1983**, *17*, 192−194.
(6) Ennever, J. F.; Speck, W. T. *Pediatr. Res.* **1983**, *17*, 234−236.
(7) Hoffmann, M. E.; Meneghini, R. *Photochem. Photobiol.* **1979**, *29*, 299−303.
(8) Edwards, A. M.; Silva, E. J., B.; Becker, M. I.; De Ioannes, A. E. *J. Photochem. Photobiol., B* **1994**, *24*, 179−186.
(9) Goodrich, R. P. *Cambridge Healthtech Institute's Sixth Annual Blood Product Safety Conference*, 2000.
(10) Silva, E.; Ugarte, R.; Andradi, A.; Edwards, A. M. *J. Photochem. Photobiol., B* **1994**, *23*, 43−48.
(11) Ono, S.; Ohkawa, K.; Hirano, H.; Obara, Y. *Int. J. Vitam. Nutr. Res.* **1986**, *56*, 259−262.
(12) Tapia, G.; Silva, E. *Radiat. Environ. Biophys.* **1991**, *30*, 131−138.
(13) Silva, E.; Salim-Hanna, M.; Edwards, A. M.; Becker, M. I.; De Ioannes, A. E.; Friedman, N. *A Light-Induced Tryptophan-Riboflavin Binding: Biological Implications*; Plenum: New York, 1991.
(14) Salim-Hanna, M.; Edwards, A. M.; Silva, E. *Int. J. Vitam. Nutr. Res.* **1987**, *57*, 155−159.
(15) Gromisch, D. S.; Lopez, R.; Cole, H. S.; Cooperman, J. M. *J. Pediatr.* **1977**, *90*, 118−122.
(16) Sisson, T. R. C.; Slaven, B.; Hamilton, P. B. *Birth Defects* **1976**, *12*, 122−133.
(17) Sisson, T. R. C. *Fed. Proc.* **1987**, *46*, 1883−1885.
(18) Silva, E.; Salim-Hanna, M.; Becker, M. I.; De Ioannes, A. *Int. J. Vitam. Nutr. Res.* **1988**, *58*, 394−401.

10.1021/ja0123711 CCC: $22.00

To understand riboflavin-protein photochemistry, the reaction of triplet flavin with indole has been examined using density functional theory (DFT) calculations[20−29] and time-resolved infrared (TRIR) spectroscopy.[30−33]

II. Density Functional Theory Calculations of Lumiflavin (LF)

In this work, LF was used as a model for RBTA in the calculations because the isoalloxazine (flavin) core, which is responsible for the flavin photochemistry, is assumed to be unperturbed by the removal of the ribityl chain.[34−36] By eliminating the ribityl chain from RB, the calculations become more practical and much faster by removing several hydrogen-bonding interactions, eliminating many possible rotamers, and significantly reducing the overall size of each calculation. Such an approach has been well utilized for computational investigations of the flavin core, and most of these studies have attempted to understand the mechanism of action of DNA photolyase.[37−44]

DNA photolyase contains a fully reduced anionic flavin moiety.[37,38,45] Upon photolysis, it transfers an electron to thymidine dimers leaving behind a neutral flavin radical. Previous computational investigations have been reported which included analysis of the spin densities, charge densities, and relative thermodynamic stabilities of flavins.[37−44] These calculations were performed at various levels of theory including UHF, ROHF, and UB3LYP. The UHF calculations on flavin radicals and radical anions suffer from considerable spin contamination ($\langle S^2\rangle \approx 1.3$) that render the resulting data suspect. Previous calculations of flavins which utilized the UB3LYP level of theory benefited from very low spin contamination, but analysis of the results was performed on the basis of a Mulliken partitioning scheme. Because data obtained via this method are often very basis set dependent[46,47] (charge density more so than spin density), Mulliken himself indicated that such a partitioning is not reliable.[46,47] Also, previous reports in which flavin calculations were performed using the B3LYP method examined only a few isomers and broad comparisons of flavin behavior and characteristics. Therefore, we present a series of density functional theory calculations on a broad family of flavins that are more reliable than previous calculations by virtue of their lower spin contamination and charge and spin densities that are based upon a non-Mulliken analysis. In addition, calculated vibrational spectra of flavin intermediates are compared to experimental time-resolved infrared spectra.

Recent studies have demonstrated that the bond dissociation enthalpies (BDEs) of polycyclic aromatic hydrocarbons (PAHs) can be accurately calculated at the B3LYP[20−22] level of density functional theory.[20,23−29] On the basis of the reported agreement between the calculated and experimental PAH BDEs, the B3LYP level was chosen for the calculations of the molecules in this system. B3LYP has the advantage over unrestricted Hartree−Fock methods for aromatic radicals as the latter may suffer from a high degree of spin contamination, whereas DFT levels of theory are usually not plagued by this problem.

All calculations were performed using Gaussian 98[48] at the Ohio Supercomputer Center. Geometries were optimized at the B3LYP/6-31G* level of theory, and single-point energies were obtained at the B3LYP/6-31+G** level with the optimized B3LYP/6-31G* geometries. Stationary points were verified to be energy minima via vibrational frequency analyses (B3LYP/6-31G*) in which all of the calculated vibrational frequencies were nonimaginary. Zero-point vibrational energy (ZPE) corrections were also obtained by the vibrational frequency calculations, and a scaling factor of 0.9804 was used.[49] Calculated vibrational frequencies were scaled by 0.9613.[50] All reaction enthalpy data represent ΔH at 0 K. Spin contamination for all of the B3LYP optimized structures was low: $0.75 < \langle S^2\rangle < 0.79$ for the doublet states and $2.0 < \langle S^2\rangle < 2.1$ for the triplet states. All spin density and charge density data were obtained by a natural population analysis (NPA) at the B3LYP/6-31G* level.[51] (NPA analysis with the 6-31+G** basis set had problems due to the inability to localize the orbitals.) Attempts to calculate the atomic charges and spin densities using Bader's atoms in molecules (AIM) methods[51−55] failed due to numerical problems in defining the atomic boundaries.

(19) La Rochette, A.; Silva, E.; Birlouez-Aragon, I.; Mancini, M.; Edwards, A. M.; Morliere, P. *Photochem. Photobiol.* **2000**, *72*, 815−820.
(20) Lee, C.; Yang, W.; Parr, R. G. *Phys. Rev. B* **1988**, *37*, 785−789.
(21) Becke, A. D. *J. Chem. Phys.* **1993**, *98*, 5648−5652.
(22) Becke, A. D. *Phys. Rev. A* **1998**, *38*, 3098.
(23) Barckholtz, C.; Barckholtz, T. A.; Hadad, C. M. *J. Am. Chem. Soc.* **1999**, *121*, 491−500.
(24) Johnson, B. G.; Gill, P. M. W.; Pople, J. A. *J. Chem. Phys.* **1993**, *98*, 5612−5626.
(25) Stephens, P. J.; Devlin, F. J.; Frisch, M. J. *J. Phys. Chem.* **1994**, *98*, 11623−11627.
(26) Bauschlicher, C. W., Jr.; Langhoff, S. R. *Mol. Phys.* **1999**, *96*, 471−476.
(27) Cioslowski, J.; Liu, G.; Moncrieff, D. *J. Org. Chem.* **1996**, *61*, 4111−4114.
(28) Cioslowski, J.; Liu, G.; Martinov, M.; Piskorz, P.; Moncrieff, D. *J. Am. Chem. Soc.* **1996**, *118*, 561−5264.
(29) Wiberg, K. B.; Cheeseman, J. R.; Ochterski, J.; Frisch, M. J. *J. Am. Chem. Soc.* **1995**, *117*, 6535−6543.
(30) Ford, P. C.; Bridgewater, J. S.; Lee, B. *Photochem. Photobiol.* **1997**, *65*, 57.
(31) Schoonover, J. R.; Strouse, G. F. *Chem. Rev.* **1998**, *98*, 1335−1355.
(32) George, M. W.; Poliakoff, M.; Turner, J. J. *Analyst* **1994**, *119*, 551−560.
(33) George, M. W.; Turner, J. J. *Coord. Chem. Rev.* **1998**, *177*, 201−217.
(34) Neither RBTA nor LF will interact with a ring nitrogen by hydrogen bonding. There may be intramolecular hydrogen bonding of a ribityl hydroxyl group with a ring nitrogen under some conditions, but no evidence of such intramolecular hydrogen bonding is seen in the X-ray crystal structure of riboflavin.
(35) Fujii, S.; Kawasaki, K.; Sato, A.; Fujiwara, T.; Tomita, K.-I. *Arch. Biochem. Biophys.* **1977**, *181*, 363.
(36) Voet, D.; Rich, A. *Proc. Natl. Acad. Sci. U.S.A.* **1971**, *68*, 1151.
(37) Lee, E.; Medvedev, E. S.; Stuchebrukhov, A. A. *J. Phys. Chem. B* **2000**, *104*, 6894−6902.
(38) Weber, S.; Mobius, K.; Richter, G.; Kay, C. W. M. *J. Am. Chem. Soc.* **2001**, *123*, 3790−3798.
(39) Meyer, M.; Hartwig, H.; Schomburg, D. *J. Mol. Struct.* **1996**, *364*, 139−149.
(40) Rotello, V. M. *Heteroat. Chem.* **1998**, *9*, 605−606.
(41) Meyer, M. *J. Mol. Struct.* **1997**, *417*, 163−168.
(42) Platenkamp, R. J.; Palmer, M. H.; Visser, A. W. G. *J. Mol. Struct.* **1980**, *67*, 45−64.
(43) Zuber, G.; Hadad, C. M., unpublished results (Ohio State University).
(44) Zheng, Y. J.; Ornstein, R. L. *J. Am. Chem. Soc.* **1996**, *118*, 9402−9408.
(45) Heelis, P. F.; Hartman, R. F.; Rose, S. D. *Chem. Rev.* **1995**, *95*, 289−297.
(46) Grier, D. D.; Streitwieser, A. *J. Am. Chem. Soc.* **1982**, *104*, 3556−3564.
(47) Mulliken, R. S.; Politzer, P. *J. Chem. Phys.* **1971**, *55*, 5135−5136.
(48) Frisch, M. J.; Trucks, G. W.; Schlegel, H. B.; Scuseria, G. E.; Robb, M. A.; Cheeseman, J. R.; Zakrzewski, V. G.; Montgomery, J. A., Jr.; Stratmann, R. E.; Burant, J. C.; Dapprich, S.; Millam, J. M.; Daniels, A. D.; Kudin, K. N.; Strain, M. C.; Farkas, O.; Tomasi, J.; Barone, V.; Cossi, M.; Cammi, R.; Mennucci, B.; Pomelli, C.; Adamo, C.; Clifford, S.; Ochterski, J.; Petersson, G. A.; Ayala, P. Y.; Cui, Q.; Morokuma, K.; Malick, D. K.; Rabuck, A. D.; Raghavachari, K.; Foresman, J. B.; Cioslowski, J.; Ortiz, J. V.; Stefanov, B. B.; Liu, G.; Liashenko, A.; Piskorz, P.; Komaromi, I.; Gomperts, R.; Martin, R. L.; Fox, D. J.; Keith, T.; Al-Laham, M. A.; Peng, C. Y.; Nanayakkara, A.; Gonzalez, C.; Challacombe, M.; Gill, P. M. W.; Johnson, B. G.; Chen, W.; Wong, M. W.; Andres, J. L.; Head-Gordon, M.; Replogle, E. S.; Pople, J. A. *Gaussian 98*, revision A.9; Gaussian, Inc.: Pittsburgh, PA, 1998.
(49) Scott, A. P.; Radom, L. *J. Phys. Chem.* **1996**, *100*, 16502−16513.
(50) Foresman, J. B.; Frisch, A. *Exploring Chemistry with Electronic Structure Methods*, 2nd ed.; Gaussian, Inc.: Pittsburgh, PA, 1996.
(51) Reed, A. E.; Weinhold, F. A.; Curtiss, L. A. *Chem. Rev.* **1998**, *98*, 899.
(52) Cioslowski, J.; Piskorz, P. *Chem. Phys. Lett.* **1996**, *255*, 315−319.
(53) Bader, R. F. W. *Atoms in Molecules − A Quantum Theory*; Clarendon Press: Oxford, 1990.
(54) Bader, R. F. W. *Acc. Chem. Res.* **1985**, *18*, 9−15.
(55) (a) Wiberg, K. B.; Rablen, P. R. *J. Comput. Chem.* **1993**, *14*, 1504−1518. (b) Bader, R. F. W. *Chem. Rev.* **1991**, *91*, 893−928.

Table 1. Comparison of Selected X-ray Crystallographic Experimental LF Bond Lengths with the Calculated Bond Lengths (B3LYP/6-31G*) of the LF Ground State, LF Triplet, and LF Radical Anion[a]

	C_2═O	C_4═O	N_1–$C_{10'}$	$C_{4'}$–$C_{10'}$	$C_{4'}$–N_5
LF (X-ray data)[b]	1.23	1.21	1.31	1.46	1.30
LF (calcd)	1.21	1.21	1.30	1.46	1.30
LF triplet (calcd)	1.22	1.22	1.32	1.41	1.36
LF radical anion (calcd)	1.23	1.23	1.32	1.42	1.36

[a] See Chart 1 for the numbering scheme. All bond distances are in angstroms. [b] Reference 56.

Chart 1

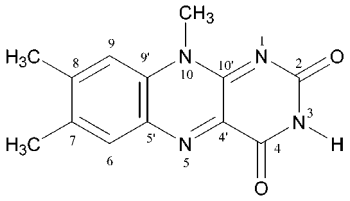

II.A. Examination of the Calculated and Experimental Bond Lengths of LF. The geometries of LF, the LF triplet, and the LF radical anion were optimized at the B3LYP/6-31G* level of theory. Selected bond lengths of the conjugated portion of the flavin ring system of the optimized LF geometries are listed in Table 1, and the atomic numbering is shown in Chart 1.

Calculations of the LF ground state indicate that the bonds between the conjugated flavin ring nitrogens (N_1 and N_5) and their adjacent carbon atoms ($C_{4'}$ and $C_{10'}$) are the same length (1.30 Å). The calculated data for LF are in good agreement with the experimental results[56] and with accepted bond distances for C═N double bonds.[57]

The calculated LF bond length between the carbon atoms within the conjugated flavin ring system ($C_{4'}$–$C_{10'}$) is significantly longer (1.46 Å) than the calculated C═N bond lengths (1.30 Å). Crystal structural data of LF agree with the calculated bond distances, and our results compare well with previous calculations of the optimized geometry of LF at various levels of theory.[37−39,44]

B3LYP/6-31+G**//B3LYP/6-31G* calculations predict that ^{3}LF* is 42.1 kcal/mol above the ground state of lumiflavin in the gas phase, which compares to the aqueous phase RB value of 49.8 kcal/mol.[58] The LF radical anion is calculated to be 45.1 kcal/mol lower in energy than the neutral LF ground state and a free electron in the gas phase.

II.B. Examination of the Calculated Bond Lengths, Change in Charge Densities, and Spin Densities of the LF Triplet State as Compared to the Ground State of LF. The calculations indicate that when LF is excited to the triplet state, the bond lengths in the flavin ring change significantly. In the excited triplet state of LF, the bonds between N_1–$C_{10'}$ and N_5–$C_{4'}$ lengthen by 0.02 and 0.06 Å, respectively, while the bond between $C_{4'}$–$C_{10'}$ shortens by 0.05 Å as compared to the calculated geometry of the LF ground state (Chart 1, Table 1).

Calculated atomic charges (B3LYP/6-31G* level) using the natural population analysis (NPA) method may not be quantitative,[54] but a qualitative comparison can be made between the same atoms in a series of related structures to determine the change in charge as a molecule is transformed from one species into another. Therefore, atomic charges of transient LF species are compared to the atomic charges in the ground state of LF in Table 2. (Complete listings of all calculated atomic charges are presented in the Supporting Information.)

Table 2. Change in NPA Atomic Charge[a] of the Triplet and Radical Anion Relative to the Ground State of LF

	N_1	N_5	$C_{4'}$	$C_{10'}$
LF	0.00	0.00	0.00	0.00
LF triplet	0.14	−0.14	−0.02	−0.06
LF radical anion	−0.06	−0.12	−0.13	−0.01
5H-LF·	0.00	−0.16	−0.06	0.00

[a] Using the B3LYP/6-31G* wave functions.

N_1 shows an increase (+0.14) in positive charge between the ground state and the triplet flavin, which is the same magnitude as the amount of negative charge gained on N_5 (−0.14). In particular, for the ground state, N_1 (−0.61) has a greater negative charge than N_5 (−0.33), and excitation of LF to the triplet state allows N_1 and N_5 to become equal in charge (−0.47).

For the calculated spin density, data are expressed as percent spin density on an atomic center as compared to the sum of all atoms in the molecule. The NPA spin density analysis shows that the two atoms with the highest percentage of the total spin density in triplet LF are N_1 and N_5 (18.2 and 15.7%, respectively). It should also be noted that there is a significant amount of spin density on $C_{4'}$ (12.4%), and almost none on $C_{10'}$ (0.3%). The calculations indicate that the LF triplet state can be best described as a biradical with unpaired electrons concentrated on N_1 and N_5.

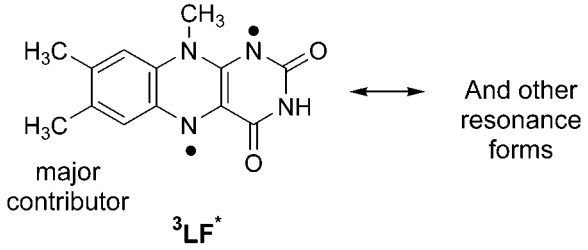

II.C. Examination of the Calculated Bond Lengths, Change in Charge Densities, and Spin Densities of the LF Radical Anion as Compared to the Ground State of LF. Upon transfer of an electron to the LF triplet state to form the LF radical anion, the C–N bond lengths remain unchanged, and the $C_{4'}$–$C_{10'}$ bond length increases by only 0.01 Å. Charge density analysis of the LF radical anion indicates a significant increase in negative charge density on N_5 and $C_{4'}$ (−0.12 and −0.13, respectively) as compared to the ground state of LF. In contrast, there is very little increase in negative charge density on N_1 and $C_{10'}$ (−0.06 and −0.01, respectively). The NPA spin density analysis of the LF radical anion indicates that there is a localization of spin density on N_5 and $C_{4'}$ (35.0 and 11.3%, respectively) with very little on N_1 and $C_{10'}$ (1.1 and 4.5%, respectively).

The data support the hypothesis that the single unpaired electron in the LF radical anion is substantially delocalized between $C_{4'}$–N_5, as indicated by the large increase in negative charge and spin density on these atoms. Because there is very

(56) Scarbrough, F. E.; Shieh, H. S.; Voet, D. *Acta Crystallogr., Sect. B* **1977**, *33*, 2512−2523.
(57) Lide, D. R. *CRC Handbook of Chemistry and Physics*, 73rd ed.; Chemical Rubber Publishing Company: Ann Arbor, 1992; pp 9.2−9.8.
(58) Murov, S. L.; Carmichael, I.; Hug, G. L. *Handbook of Photochemistry*, 2nd ed.; Marcel Deeker Inc.: New York, 1993.

Table 3. Comparison of Calculated[a] and Experimental[b] Carbonyl Vibrational Frequencies in the LF Ground State, LF Triplet, and LF Radical Anion

	calculated LF frequencies (cm^{-1})		experimental $RB(OAc)_4$ frequencies (cm^{-1})
ground state (KBr)			1660, 1714, 1749
ground state (TRIR)	1736 (100)	1744 (33)	1684, 1716, 1756
triplet (TRIR)	1634 (100)	1682 (100)	1652
radical anion (TRIR)	1679 (55)	1687 (100)	1636

[a] All values are calculated at the B3LYP/6-31G* level of theory and scaled by 0.9613. Relative intensities are listed in parentheses. [b] Experimental values obtained from $RB(OAc)_4$ by TRIR differential spectra in CD_3CN or by solid $RB(OAc)_4$/KBr pellet as noted.

Table 4. Comparison of Selected Calculated[a] and Experimental[b] C═N Vibrational Frequencies in the LF Ground State, LF Triplet, and LF Radical Anion

	calculated LF frequencies (cm^{-1})		experimental $RB(OAc)_4$ frequencies (cm^{-1})
ground state (KBr)			1541, 1582
ground state (TRIR)	1538 (75)	1575 (113)	1548, 1588
triplet (TRIR)	1466 (100)	1559 (85)	1436, 1484
radical anion (TRIR)	1505 (42)	1523 (33)	1500, 1524

[a] All values are calculated at the B3LYP/6-31G* level of theory and scaled by 0.9613. Relative intensities are listed in parentheses. [b] Experimental values obtained from $RB(OAc)_4$ by TRIR differential spectra in CD_3CN or by solid $RB(OAc)_4$/KBr pellet as noted.

little difference in charge density between the LF radical anion and the ground state of LF on N_1 and $C_{10'}$, as well as very little spin density, the bond between these atoms can be viewed as being similar to that of the ground-state flavin. If charge density is a prediction of the preferred site of ionic reactivity, then one can conclude that the site of "predicted kinetic" protonation of the LF radical anion will be at N_5 or $C_{4'}$ on the basis of the following resonance structures. Important resonance structures of the LF radical anion are presented below on the basis of the calculated charge and spin density data. Significant delocalization of both the charge and the spin density exists throughout the *o*-xylyl ring and the amide system.

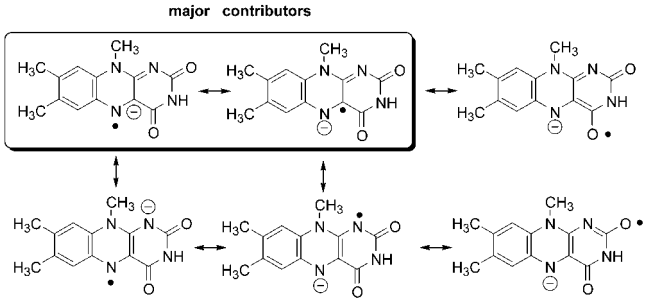

II.D. Calculated Vibrational and TRIR Spectra of LF, LF Triplet, and the LF Radical Anion. DFT calculations were also used to predict the vibrational spectra of lumiflavin, triplet lumiflavin, and the lumiflavin radical anion (Tables 3 and 4). The vibrational spectrum of the related flavin, riboflavin tetraacetate (RBTA), was obtained by traditional IR spectroscopy and that of the transient species derived from it by time-resolved infrared (TRIR) spectroscopy.[59,60] The TRIR spectra are difference spectra comparing infrared absorption post- and pre-laser excitation.

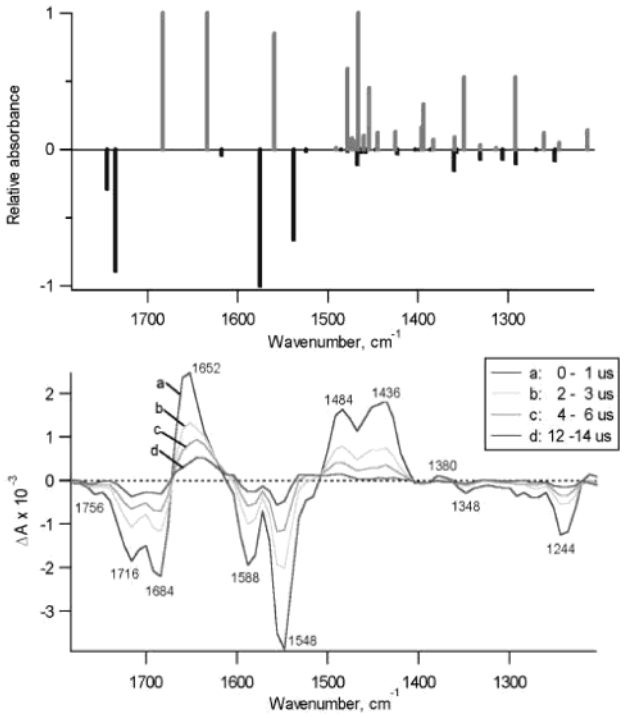

Figure 1. Calculated (top) and experimental (bottom) difference spectra of the transformation of LF (negative peaks) into the LF triplet (positive peaks). Experimental data were obtained by 355 nm laser flash photolysis (LFP) of RBTA in CD_3CN. The calculated B3LYP/6-31G* vibrational frequencies have been scaled by 0.9613.

Experimentally, RBTA was used instead of RB or LF because the latter two flavins have poor solubility in acetonitrile, a solvent with wide spectral windows in the infrared. A comparison of the TRIR spectra of RBTA with the calculated vibrational spectra of various LF species can be made since the difference spectra reveal information about only those molecular features that have undergone photochemical transformation, and these will be dominated by the flavin ring system.

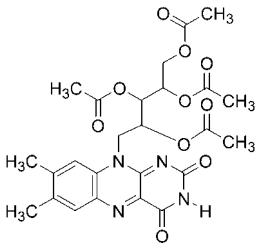

Flash photolysis (355 nm, ND-YAG laser, 0.5−0.7 mJ/pulse, 97 Hz repetition) of RBTA in deoxygenated acetonitrile-d_3 produced the difference spectra shown in the bottom of Figure 1. The negative peaks are due to depletion of ground-state RBTA. The positive peaks are due to the presence of a transient intermediate. The transient has a lifetime of 2 μs (Figure 2),

(59) Yuzawa, T.; Kato, C.; George, M. W.; Hamaguchi, H. *Appl. Spectrosc.* **1994**, *48*, 684−690.
(60) Iwata, K.; Hamaguchi, H. *Appl. Spectrosc.* **1990**, *44*, 1431.

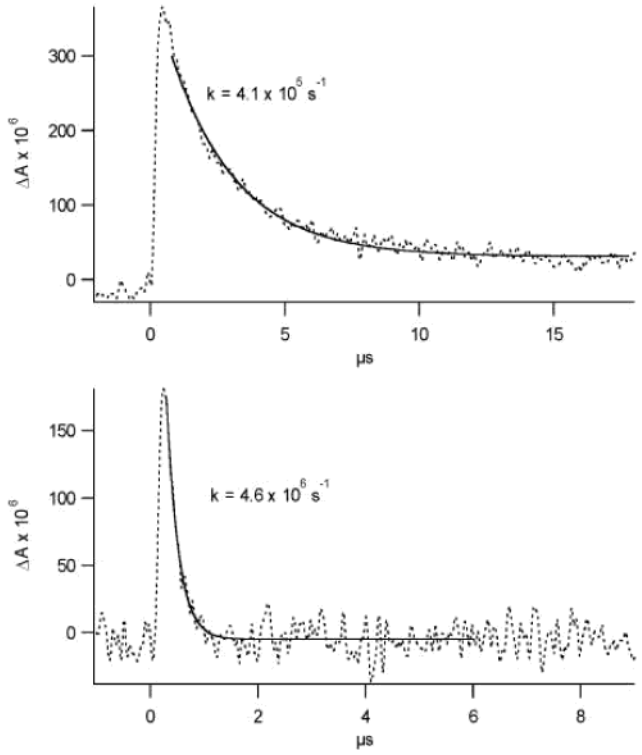

Figure 2. The decay of transient absorption at 1656 cm^{-1} following LFP (355 nm) of RBTA in CD_3CN saturated with argon (top) and oxygen (bottom), respectively.

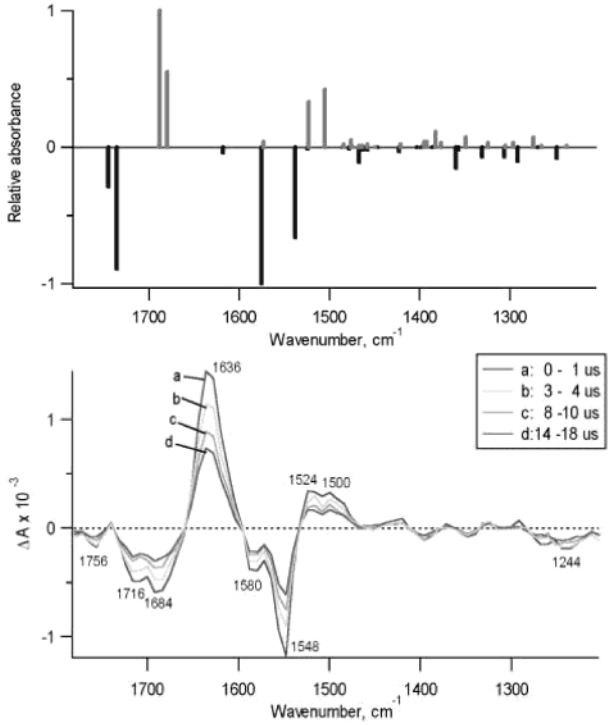

Figure 3. Calculated (top) and experimental (bottom) difference spectra from the transformation of LF (negative peaks) into the LF radical anion (positive peaks). Experimental data were obtained by 355 nm laser flash photolysis (LFP) of RBTA with NaI in CD_3CN. The calculated B3LYP/6-31G* vibrational frequencies have been scaled by 0.9613.

and as it decays, the spectrum of ground-state RBTA recovers with the same time constant. The presence of oxygen dramatically shortens the lifetime of the transient (Figure 2, bottom). Given these observations, the large quantum yield of triplet formation of riboflavin,[2,3] and the good agreement between the calculated spectrum of triplet lumiflavin[61] (Figure 1, top) and the transient spectrum derived from RBTA, the transient is assigned to triplet RBTA (^{3}RBTA*). The predicted bands of ^{3}RBTA* of moderate intensity between 1300 and 1400 cm^{-1} are not observed. The calculations do not predict the intensities of all bands correctly since Fermi resonance, which is observed in the experimental spectra, is not included in the calculated spectra.

Iodide ion is expected to quench ^{3}RBTA* by electron transfer to form the flavin radical anion and an iodine atom.[2,3] Indeed, flash photolysis of RBTA in CD_3CN containing 20 mM sodium iodide produces the transient spectrum of Figure 3. The prominent peaks in the carbonyl region of the TRIR spectra differ significantly in the presence (1636 cm^{-1}, Figure 3) and absence (1652 cm^{-1}, Figure 1) of sodium iodide, and the intense bands of the triplet flavin between 1400 and 1500 cm^{-1} are no longer present. The transient observed in the presence of sodium iodide has a lifetime of greater than 10 μs and is attributed to the RBTA radical anion. The rate of disappearance of the radical anion is equal to the rate of recovery of the photobleached TRIR spectrum of ground-state RBTA. It seems likely then that the RBTA radical anion reacts with iodine atom to re-form RBTA and iodide ion.

(61) Although the bands at 1300 and 1350 cm^{-1} do not appear to agree well with the experimental spectra, it is believed that the calculation does not represent these intensities accurately. The calculations also do not consider Fermi resonance, which may affect the intensities observed in the experimental results.

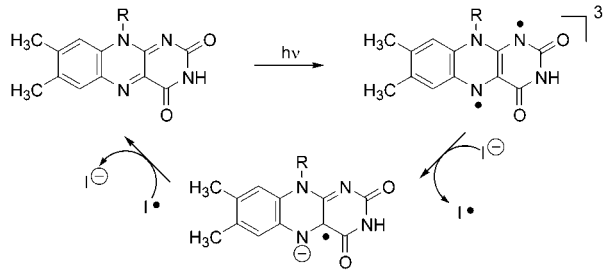

This is a second-order process; thus the reaction rate continuously decreases and is not complete over the time scale of observation shown. The spectrum does decay to baseline on the millisecond time scale. No additional TRIR bands other than those of ground-state RBTA are formed as the RBTA radical anion decays.

As expected, the RBTA radical anion will react with a proton donor. The lifetime of the transient is shortened by the presence of a proton donor (NH_4Cl) (Figure 4, top, a, b). As the RBTA radical anion is quenched by NH_4Cl, a growth in transient absorption is observed at 1660 cm^{-1} (Figure 4, top, c). The spectrum observed in the presence of NH_4Cl (Figure 4, bottom, e) is attributed to a neutral flavin radical formed by protonation of the flavin radical anion (Figure 4, bottom, d). Several sites of protonation of the RBTA radical anion are possible which result in the formation of various isomeric radicals.

II.E. Calculated Thermodynamic Stabilities of the Isomeric Neutral Radicals Formed upon Protonation of the Flavin Radical Anion. Six positions (1, 2-OH, 4-OH, 4′, 5, and 10′, Figure 5) were considered potential sites of protonation of the flavin radical anion because of the atomic electronegativities and their location within the conjugated flavin core. The

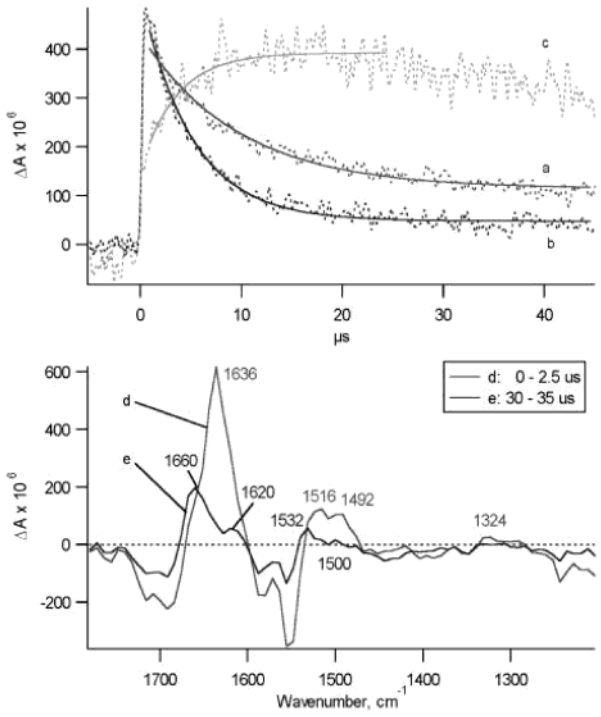

Figure 4. The decay of RBTA radical anion (1636 cm^{-1}) in the (top, a) absence of NH_4Cl and (top, b) in the presence of NH_4Cl, the growth of transient absorption (1660 cm^{-1}) in the presence of NH_4Cl and NaI (top, c), and the TRIR spectrum produced upon LFP (355 nm) of RBTA in CD_3CN with the presence of NH_4Cl and NaI (bottom).

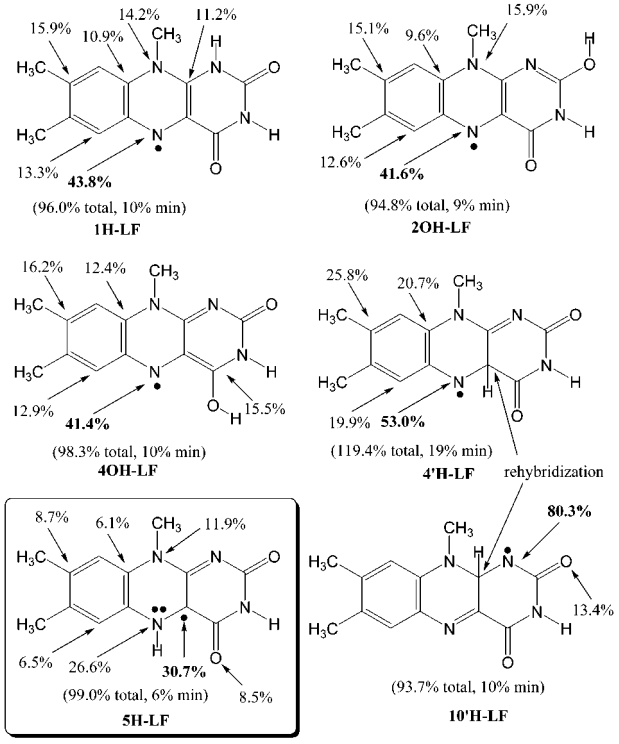

Figure 5. Major resonance contributors of various H-LF• radicals based upon spin density analysis. Numerical values indicate percent spin density (radical character) at that atomic center relative to the sum of the spin on all atoms in that molecule.[67]

energy of the most stable structure is defined as 0.0 kcal/mol. Figure 5 depicts each radical in its major resonance form along with its spin density distribution. The relative energies of these radicals are given in Table 5.

Table 5. Relative Stabilities of Selected H-LF• Radicals[a]

isomer[b]	B3LYP/6-31G*	B3LYP/6-31+G**//B3LYP/6-31G*
1H-LF•	8.4	8.6
2OH-LF•	12.3	11.2
4OH-LF•	9.4	8.4
4′H-LF•	23.8	25.3
5H-LF•	0.0	0.0
10′H-LF•	49.3	51.1

[a] Relative energies as ΔH (0 K) in kcal/mol using the scaled ZPE from the B3LYP/6-31G* level of theory. [b] See Figure 5 for structures.

Table 5 reveals that 5H-LF• is the most stable isomer, which is more than 8 kcal/mol lower in energy as compared to the next most stable isomer. The isomers formed by the acceptance of a proton at the N_1, 2-OH, and 4-OH positions all have similar calculated energies, within 4 kcal/mol. The radicals resulting from the addition of a proton to a carbon center (4′ and 10′) are both very high in energy (25 and 51 kcal/mol, respectively) as compared to 5H-LF•.

The simplest structures to explain with regard to spin density are the 4′H-LF• and 10′H-LF• radicals. Both of these structures have two striking features in common. The first feature is that since the reaction center is at carbon, the resulting hybridization is sp^3, instead of sp^2. This rehybridization requires energy and will therefore result in a higher energy for these two structures. Second, the greatest spin density observed in these isomers is at a nitrogen atom adjacent to the site of reaction. In 10′H-LF•, the spin density is almost entirely localized at N_1 (80.3%). No other structure in this family of isomers has an atom with such a large value of the spin density. Similarly, 4′H-LF• is also very high in energy, but not as high as 10′H-LF•. The added stability of the 4′H-LF• radical is caused by the increased delocalization of the resulting radical.[23] Because the radical center lies at a benzylic (anilinic) position, the electron can be delocalized throughout the aromatic ring, which causes the spin density on N_5 to be lower in 4′H-LF• (53.0%) as compared to the spin density of N_1 (80.3%) in 10′H-LF•.

Examination of the 1H-LF•, 2OH-LF•, and 4OH-LF• radicals reveals a strong similarity in the contributing resonance structures of these three isomers. All three radicals have the largest spin density (>40.0%) located at N_5, and, therefore, the radical is also delocalized throughout the adjacent aromatic *o*-xylyl ring. Because the three structures appear to have very similar resonance structures, it is not surprising that their calculated energies are within a few kcal/mol. The only noteworthy difference between these three structures is that there is significant spin density on $C_{10'}$ in 1H-LF• and 2OH-LF• (11.2 and 9.4%, respectively), while there is almost none at that position in 4OH-LF• (2.6%). This is due to the inability to form a resonance structure with a radical center on that atom when one starts from the hydrogen addition at the carbonyl oxygen at position $C_{4'}$.

The most interesting spin density analysis belongs to the 5H-LF• radical structure, which is also the lowest in energy. Besides delocalizing the odd electron through a conjugated system as seen in the other structures, the radical is somewhat delocalized on two adjacent atoms. The highest spin density (30.7%) is observed on $C_{4'}$, but there is also a large amount (22.6%) of spin density on N_5. The $C_{4'}$ carbon atom retains its planarity from the parent structure and therefore has a "pure" p orbital.

Table 6. Calculated[a] Carbonyl Vibrational Frequencies of H-LF• Radical Species

	calculated carbonyl vibrational frequencies	
1H-LF•	1766 (100)	1738 (53)
2OH-LF•	1609 (100)	1736 (99)
4OH-LF•	1548 (47)	1745 (100)
4′H-LF•	1747 (100)	1773 (41)
5H-LF•	1681 (63)	1724 (100)
10′H-LF•	1668 (100)	1746 (70)

[a] All values (in cm^{-1}) were calculated at the B3LYP/6-31G* level of theory and scaled by 0.9613. Relative intensities are provided in parentheses.

Both $C_{4'}$ and N_5 are sp^2 hybridized, and each atom has one electron in its p orbital. The remaining odd electron can then be delocalized throughout the adjacent π system (from N_5) or through the heteroatomic ring (from $C_{4'}$). This accounts for the retained geometry at $C_{4'}$ and also the nearly equal spin density at these two atomic centers.

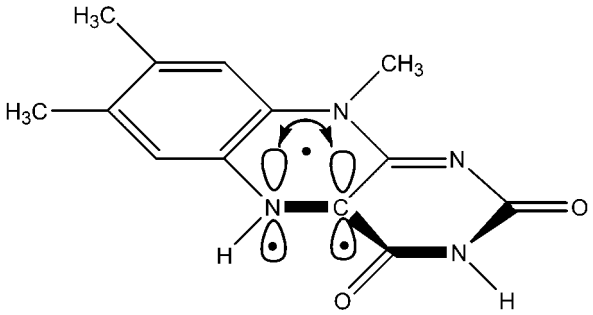

If this hypothesis is correct, then it should be evident upon examination of the change in the atomic charge of these atoms in comparison to the parent compound. If the odd electron is shared between these two atoms, there will be an increase in the amount of negative charge on $C_{4'}$ since one possible resonance structure has a lone pair of electrons occupying the p orbital on $C_{4'}$. As seen in Table 2, there is a marked increase in the amount of negative charge that is gained on atoms $C_{4'}$ and N_5 in 5H-LF• as compared to the ground state of LF. This further confirms the hypothesis for the radical being delocalized between N_5 and $C_{4'}$. It is interesting to note that the thermodynamically favored flavin radical is also the "expected" kinetically favored radical formed by protonation of the atom with the largest negative charge on the radical anion. This radical has been characterized by ESR spectroscopy and is often represented as the equivalent of 5H-LF• on the basis of the agreement of the hyperfine coupling constants with calculated values.[38,62,63]

Table 6 lists the vibrational frequencies of the carbonyl region of each neutral radical considered in Figure 5. The carbonyl vibration of 5H-LF•, the kinetically and thermodynamically favored flavin radical, is in best agreement with the experimental spectrum (Figure 4d) observed upon flash photolysis of RBTA in the presence of NaI and NH_4Cl. While the vibrational frequencies of 10′H-LF• appear reasonable, the calculated relative energy (~50 kcal/mol) suggests that 10′H-LF• is not

Scheme 1

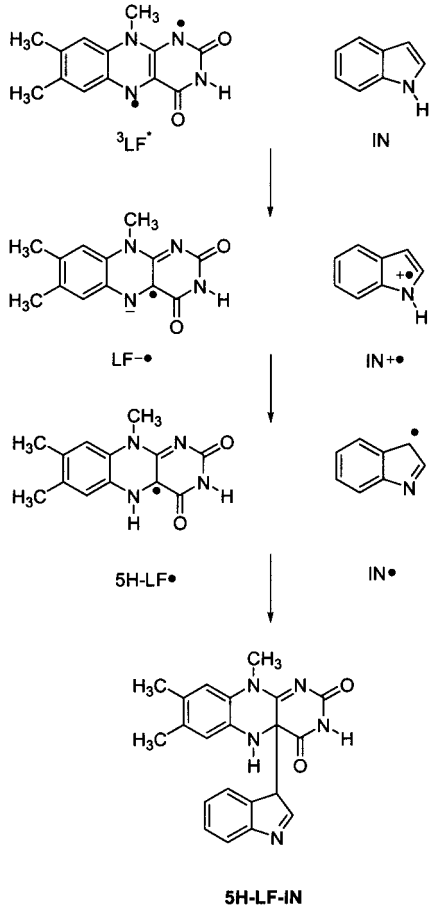

the carrier of the transient absorbing at 1660 cm^{-1}. Thus, the carrier of the transient spectrum (Figure 4d) is attributed to 5H-LF• on the basis of the DFT calculations and TRIR spectroscopy.

II.F. TRIR Spectroscopy of RBTA and Indole. Indole (IN) is expected to undergo electron-transfer reaction with triplet flavins (Scheme 1) to form a radical ion pair.[2,3] Rapid proton transfer within the radical ion pair will lead to the 5H-LF•/IN• radical pair.

Flash photolysis of RBTA in deoxygenated CD_3CN containing 20 mM indole produces the transient spectrum of Figure 6 (top). The position of the transient carbonyl band at 1660 cm^{-1} resembles that of ^{3}RBTA* (1652 cm^{-1}) in Figure 1, but lacks the intense C═N bands of ^{3}RBTA* at 1484 and 1436 cm^{-1}. Furthermore, the lifetime of the species absorbing at 1660 cm^{-1} is about 5 times longer than that of ^{3}RBTA*. The TRIR spectrum in the presence of indole most resembles the radical spectrum observed upon flash photolysis of RBTA in the presence of NaI and NH_4Cl (Figure 4, bottom). Thus, the carrier of the 1660 cm^{-1} band is attributed to a neutral flavin radical derived from protonation of the RBTA radical anion.

We predict that the riboflavin-indole adducts will have the structure shown in Scheme 1. In fact, Hemmerich et al. have isolated adducts of 3-methyllumiflavin and cyclopentadiene,[64] with very similar structures. Heelis, Hartman, and Rose have observed $C_{4'}$ photoadducts of LF with alcohols and ethers.[45] We predict that the flavin-tryptophan adducts observed with

(62) Kay, C. W. M.; Feight, R.; Schultz, K.; Sadewater, P.; Sancar, A.; Bacher, A.; Mobius, K.; Richter, G.; Weber, S. *Biochemistry* **1999**, *38*, 16740−16748.
(63) Kurreck, H.; Bock, M.; Bretz, N.; Elsner, M.; Kraus, H.; Lubitz, W.; Muller, F.; Geissler, J.; Kroneck, P. M. H. *J. Am. Chem. Soc.* **1984**, *106*, 737−746.
(64) Bruestlein, M.; Knappe, W. R.; Hemmerich, P. *Angew. Chem., Int. Ed. Engl.* **1971**, *10*, 804−806.

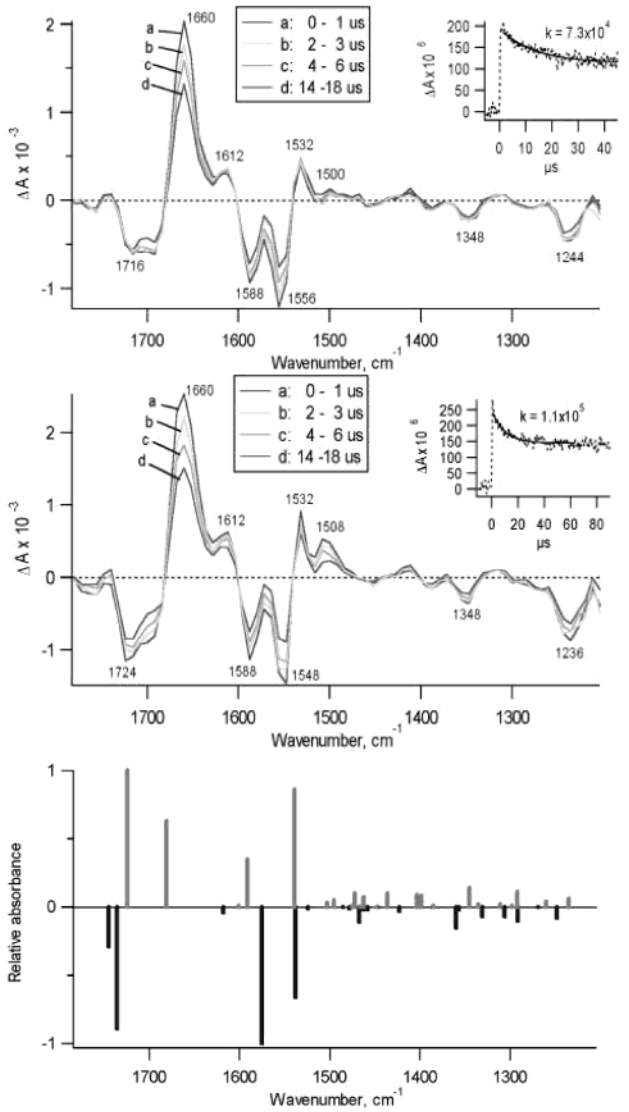

Figure 6. The TRIR spectrum produced upon LFP (355 nm) of RBTA in CD_3CN in the presence of 20 mM indole (top), TRIR spectrum produced upon LFP (355 nm) of RBTA in CD_3CN in the presence of 20 mM *p*-cresol (middle), and the calculated vibrational spectrum of 5H-LF• radical (positive peaks) and LF (negative peaks) (bottom). The calculated B3LYP/6-31G* vibrational frequencies have been scaled by 0.9613.

ocular proteins and albumin[10−15] are formed by the analogous electron-transfer, proton-transfer, and radical pair recombination mechanism.

Finally, we note that flash photolysis of RBTA and 20 mM *p*-cresol also generates the transient IR spectrum of 5H-RBTA• (Figure 6, middle) by sequential electron and proton transfer.

The TRIR spectra obtained in the presence of NaI and NH_4Cl, *p*-cresol, and indole are very similar. This indicates that the spectral features are derived from the flavin core and from neither an indolyl (IN•) nor phenoxyl (P•) radical.

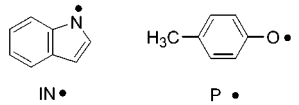

IN• P •

The IR spectra of IN• and P• were calculated using the B3LYP/6-31G* level of theory and are provided in the Supporting Information. The calculated vibrational spectra of

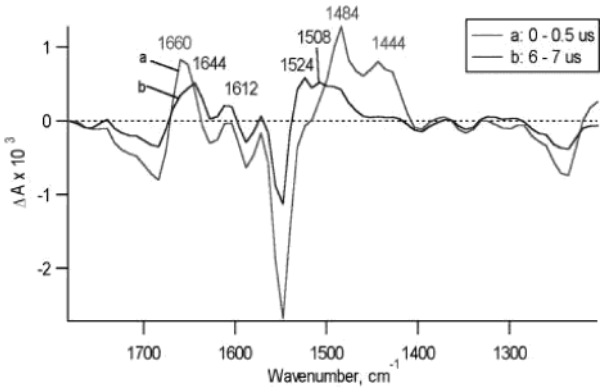

Figure 7. The TRIR spectrum produced upon LFP (355 nm) of RBTA in CD_3CN with the presence of tri-*n*-butyl tin hydride.

IN• and P• do not coincide with the TRIR bands of Figures 4 and 6, pointing again to a flavin origin of these vibrations.

A peak at 1508 cm^{-1} is observed in the presence of *p*-cresol, but not in the presence of indole. The band at 1508 cm^{-1} has the same lifetime as the other TRIR bands, suggesting it originates from the same neutral flavin radical. *p*-Cresol (1516 cm^{-1}) and its related phenoxy radical (1500 cm^{-1}) absorb in this vicinity (Supporting Information). The ground-state vibrational spectrum of indole was recorded with the TRIR spectrometer and is given in the Supporting Information. Indole absorbs weakly at 1511 cm^{-1}. We believe that the weak 1508 cm^{-1} band has its shape determined by large precursor bleaching, and for this reason we attach little significance to the variation of its shape with indole and *p*-cresol.

RBTA was flashed in the presence of 10 mM tri-*n*-butyl tin hydride, a quencher with an easily abstracted hydrogen atom that is not a particularly good electron donor. This provides the opportunity for direct hydrogen transfer to triplet RBTA without an intervening electron-transfer step. The TRIR spectrum, given in Figure 7, contains the characteristic radical band at 1660 cm^{-1}. The TRIR difference spectrum, given in Figure 7, contains a band at 1644 cm^{-1}. This band is attributed to 5H-RBTA• even though it is shifted from 1660 cm^{-1} as observed in the presence of cresol and indole. We attribute this "apparent" shift as before to differences in the ground-state spectra.

III. Conclusions

Density functional theory has been used to calculate the minimum energy geometries of lumiflavin, its triplet state, and its radical anion. The spin and charge distribution of the latter two species were also calculated. The radical anion has its greatest charge density at N_5 and $C_{4'}$ which is predicted to be the site of kinetic protonation. Protonation of the radical anion forms a neutral radical. The energies of six neutral flavin radicals were calculated, and the most stable radical results from protonation of N_5 of the radical anion. The time-resolved infrared (TRIR) spectra of triplet riboflavin tetraacetate (RBTA), its radical anion, and neutral radical were obtained by flash photolysis (355 nm) of RBTA, RBTA with sodium iodide, and RBTA with indole or *p*-cresol in deoxygenated acetonitrile-d_3. The TRIR spectra are in excellent agreement with the calculated vibrational spectra. The adducts of riboflavin and proteins at tryptophan residues are postulated to derive from an electron-

transfer, proton-transfer, and radical pair recombination mechanism.

IV. Experimental Section

Time-Resolved Infrared (TRIR) Studies. TRIR experiments were conducted with a JASCO TRIR-1000 dispersive-type IR spectrometer with 16 cm^{-1} resolution following the method described in the literature.[30−33,59,60,65] Briefly, a reservoir of deoxygenated sample solution (20 mL 2.5 mM RBTA in CH_3CN or CD_3CN with or without the desired amount of NaI, NH_4Cl, indole, *p*-cresol, or tri-*n*-butyl tin hydride) was continuously circulated between two calcium fluoride salt plates with a 0.5 mm path length. The sample was excited by 355 nm laser pulses of an Nd:YAG laser (97 Hz repetition rate, 0.5−0.7 mJ/pulse power), which is crossed with the broadband output of a $MoSi_2$ IR source (JASCO). The intensity change of the IR light induced by photoexcitation is monitored as a function of time by an MCT photovoltaic IR detector (Kolmar Technologies, KMPV11-1-J1), with a 50 ns rise time, amplified with a low noise NF Electronic Instruments 5307 differential amplifier, and digitized with a Tektronix TDS784D oscilloscope. The TRIR spectrum is analyzed by the IGOR PRO program (Wavemetrics Inc.) in the form of a difference spectrum:

$$\Delta A_t = -\log(1 + \Delta I_t/I)$$

where ΔI_t is the intensity change induced by photoreaction at time t, and I is the IR intensity for the sample without photoexcitation. Thus, depletion of reactant and formation of transient intermediates or products lead to negative and positive signals, respectively.

2′,3′,4′,5′-Tetraacetylriboflavin (riboflavin tetraacetate, RBTA) was synthesized according to the method of McCormick.[66] All other reagents were purchased from commercial suppliers and used as received.

(65) Toscano, J. P. *Adv. Photochem.* **2001**, *26*, 41.
(66) McCormick, D. B. *Heterocycl. Chem.* **1970**, *7*, 447.

Acknowledgment. The authors are indebted to the NSF (C.M.H., CHE-9733457) for financial support, and CHE-9808052 for funding of the TRIR spectrometer. We also acknowledge the Ohio Supercomputer Center for generous allocations of computational resources. One of us (M.-L.T.) gratefully acknowledges a Presidential Fellowship of The Ohio State University.

Supporting Information Available: Computational data including calculated energy summaries, bond lengths, charge density, spin density, and calculated vibrational spectra. Transient UV−vis and IR spectra of *p*-cresol with di-*tert*-butylperoxide and FTIR spectra of RBTA, *p*-cresol, and indole (PDF). This material is available free of charge via the Internet at http://pubs.acs.org.

JA0123711

(67) The spins on the atoms are expressed as the spin density on that atom as a percentage of the total excess spin in that molecule. This is done instead of displaying the actual $\alpha-\beta$ spin value as to allow the comparison of a radical anion and a triplet, which do not have the same number of unpaired electrons. Because of the nature of calculating spin densities, an unpaired electron is given an α spin state. Therefore, the sum of all the spin density of all atoms in a radical would then add up to that for a single unpaired electron, 1. In some cases, atoms are calculated to have spin densities other than a positive number or zero. Therefore, when the atoms have a positive β spin, additional α spin must be present in the molecule to account for this extra β spin. When this happens, the sum of the percent spin density of all the atoms in the molecule with a positive spin density ($\alpha-\beta > 0$) will add up to greater than 100%, since some atoms will have a negative spin density ($\alpha-\beta < 0$). This is done to help clarify data such as that found on 4′H-LF in Figure 5, where the sum of the listed percent spins is well above 100%. To help clarify this potential confusing issue, the total percent spin of the atoms indicated with a value is listed as "% total" and of all the indicated atoms having a percent spin which is above a threshold, "% min".